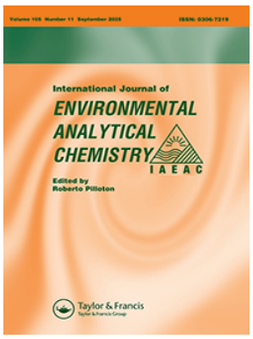

International Journal of Environmental Analytical Chemistry

ISSN: 0306-7319 (Print) 1029-0397 (Online) Journal homepage: www.tandfonline.com/journals/geac20

Assessing the radiological hazards due to radionuclides in sediments and tailings around Kilembe copper mines, Western Uganda

Evarist R. S. Turyahabwa, Farooq Kyeyune, Eric Mucunguzi, Akisophel Kisolo & Manny Mathuthu

To cite this article: Evarist R. S. Turyahabwa, Farooq Kyeyune, Eric Mucunguzi, Akisophel Kisolo & Manny Mathuthu (2025) Assessing the radiological hazards due to radionuclides in sediments and tailings around Kilembe copper mines, Western Uganda, International Journal of Environmental Analytical Chemistry, 105:11, 2587-2604, DOI: 10.1080/03067319.2024.2325110

To link to this article: https://doi.org/10.1080/03067319.2024.2325110

INTERNATIONAL JOURNAL OF ENVIRONMENTAL ANALYTICAL CHEMISTRY
2025, VOL. 105, NO. 11, 2587–2604
https://doi.org/10.1080/03067319.2024.2325110

Assessing the radiological hazards due to radionuclides in sediments and tailings around Kilembe copper mines, Western Uganda

Evarist R. S. Turyahabwa [a], Farooq Kyeyune [a], Eric Mucunguzi[a], Akisophel Kisolo[b] and Manny Mathuthu [c]

[a]Department of Physics, Faculty of Science, Kyambogo University, Kampala, Uganda; [b]The Uganda Atomic Energy Council (UAEC), Kampala, Uganda; [c]Center for Applied Radiation Science and Technology (CARST), North-West University (Mafikeng Campus), Mmabatho, South Africa

ABSTRACT

Copper mining in Kilembe Valley, Western Uganda, between 1956 and 1982 resulted in multiple tailing sites, raising concerns about potential increases in the natural background radiation. In this study, the radioactivity concentrations of ^{226}Ra, ^{232}Th, and ^{40}K in 31 sediments and tailing samples from the Kilembe copper mines area were determined using HPGe-based gamma spectrometry. The mean activity concentrations of ^{226}Ra, ^{232}Th, and ^{40}K in sediment samples were 38.6 ± 8.9, 37.4 ± 7.8, and 708.0 ± 147.3 Bq kg^{-1}, respectively. While in tailing samples, the mean values were 171.3 ± 31.7, 34.8 ± 14.9, and 792.4 ± 208.2 Bq kg^{-1}, respectively. These values exceeded global averages of 35, 30, and 400 Bq kg^{-1} for ^{226}Ra, ^{232}Th, and ^{40}K, respectively. To assess the radiological hazards due to radionuclides in sediments and tailings, several parameters such as the radium equivalent activity (Ra_{eq}), external hazard index (H_{ex}), internal hazard index (H_{in}), gamma representative index (I_γ), absorbed dose rate (D), total annual effective dose (E_{tot}), and total excess lifetime cancer risk ($ELCR_{tot}$) were determined. In sediments, most of these hazard parameters were above the world's average values, except Ra_{eq}, I_γ, H_{ex}, and H_{in}. While in tailings, all the hazard parameters surpassed the global average values except Ra_{eq} and H_{ex}. Pearson correlation coefficient and hierarchical cluster analysis showed that ^{226}Ra was the main contributor to the assessed radiological hazards. The study suggests potential radiological risks linked to natural radioactivity from sediments and mine tailings, especially when used as building materials.

ARTICLE HISTORY
Received 2 January 2024
Accepted 21 February 2024

KEYWORDS
Activity concentrations; Kilembe copper mines; natural radionuclides; radiological hazard parameters; sediments; tailings

1. Introduction

Naturally occurring radionuclides and their accompanying radioactivity have existed since the formation of the universe [1]. This enduring existence suggests that life has evolved in the presence of radionuclides, some of which have undergone complete decay. However,

CONTACT Evarist R. S. Turyahabwa silvertury78@gmail.com
Supplemental data for this article can be accessed online at https://doi.org/10.1080/03067319.2024.2325110.

those with longer half-lives, such as ^{238}U, ^{232}Th, and ^{40}K, and their daughter isotopes that constitute the primordial radionuclides still exist in many environmental matrices at varying concentrations [2]. Sources of natural radionuclides include rocks, soil, sediments, plants, water, and air [3]. Human exposure to radionuclides can occur through various pathways, including inhalation (mostly radon and its progenies), ingestion (via food and water consumption), medical procedures, and dermal exposure. The radiation dose received by an individual depends on the concentration of natural radionuclides, duration of exposure, route of exposure, and the lifestyle of the exposed population. Chronic exposure to high gamma radiation doses can increase the risk of lung and kidney cancers as well as other health problems [4]. Therefore, measuring the concentration of natural radionuclides in the environment is essential to evaluate the potential radiological health risks to the public.

Anthropogenic processes such as mining can influence the distribution and concentration of natural radioactivity in the environment, raising human health concerns [5]. Mining activities involve the production of large quantities of waste material known as mine tailings. Over time, these materials undergo weathering and erosion, forming sediments that eventually settle out of moving water in rivers, lakes, or oceans. The sediments mainly consist of silt, sand, and gravel and these are commonly used as mixing materials in construction. Mine tailings, especially from copper [6], iron [7], and gold [8] ores, have the potential to partially replace sand or cement in mortar and concrete. Despite these economic benefits, sediments and tailings contain natural radionuclides of varying concentrations depending on the region's geological formations, mineral composition, physical properties of the environmental matrices, and geographical conditions [9,10]. Accordingly, numerous studies across different regions of the world have been undertaken to analyse the concentration of radionuclide (^{238}U, ^{226}Ra, ^{232}Th, and ^{40}K) and their radiological implications in sediments [11–13] and mine tailings [14–16]. In some of the studies, the radionuclide concentrations and the associated radiological hazards higher than the world average values were reported in river sediments in Vietnam [13] and gold mine tailings in South Africa [14]. Hence, evaluating the concentration of radionuclides in these materials is imperative to assess the potential health effects on human exposure.

Copper mining in Kilembe, situated in Kasese District, Western Uganda, occurred between 1956 and 1982. This subsequently resulted in the creation of multiple mine tailing sites, causing environmental pollution [17]. The River Nyamwamba, fed by melting glaciers from the Rwenzori Mountains, frequently floods the Kilembe Valley, particularly during rainy seasons. Consequently, vast amounts of sediments and degraded soil containing tailing waste end up in the gardens and homes of the residents. These residents use the sediments and tailings from the gardens and the banks of River Nyamwamba for various purposes, including making bricks for house construction and cleaning household utensils. However, knowledge of radioactivity concentrations of ^{226}Ra, ^{232}Th, and ^{40}K in sediments and non-uranium mine tailings is still scarce, especially in developing countries like Uganda. Moreover, information about the radiological health hazards associated with exposure to radiations from sediments and tailings in the Kilembe copper mines area remains largely unknown.

Therefore, this study aimed to assess the radiological hazards due to natural radionuclides in sediments and mine tailings collected along River Nyamwamba in the Kilembe

Valley, Western Uganda. The radioactivity concentrations of ^{226}Ra, ^{232}Th, and ^{40}K were analysed using gamma-ray spectrometry and the analytical results were used to assess the radiological hazard parameters. In addition, multi-statistical analyses were implemented to exhibit the correlations between the measured radionuclide concentrations and radiological hazard parameters. The results of this study are expected to serve as a reference for further research on radiological hazard assessments and provide crucial insights into formulating radiation protection policies.

2. Materials and methods

2.1. Study area

The area of study is situated within the geographical coordinates spanning 0° 13′ 54′ and 0° 11′ 4′ north latitudes and 30° 0′ 12′ and 30° 1′ 25′ east longitudes, which includes Kilembe mines, the tailing sites, and River Nyamwamba, as shown in Figure 1. The Kilembe mines area is located at 0° 12′ 17″ north latitude and 30° 0′ 9″ east longitude, approximately 10 km from Kasese town, on the foothills of the Rwenzori Mountains in Western Uganda. Kilembe Mines is the largest copper mine in Uganda. Although legal mining activities ceased in 1982, the government of Uganda has plans to reopen the mine in the future. Within the Kilembe mines area are five copper mine tailing sites, with the largest

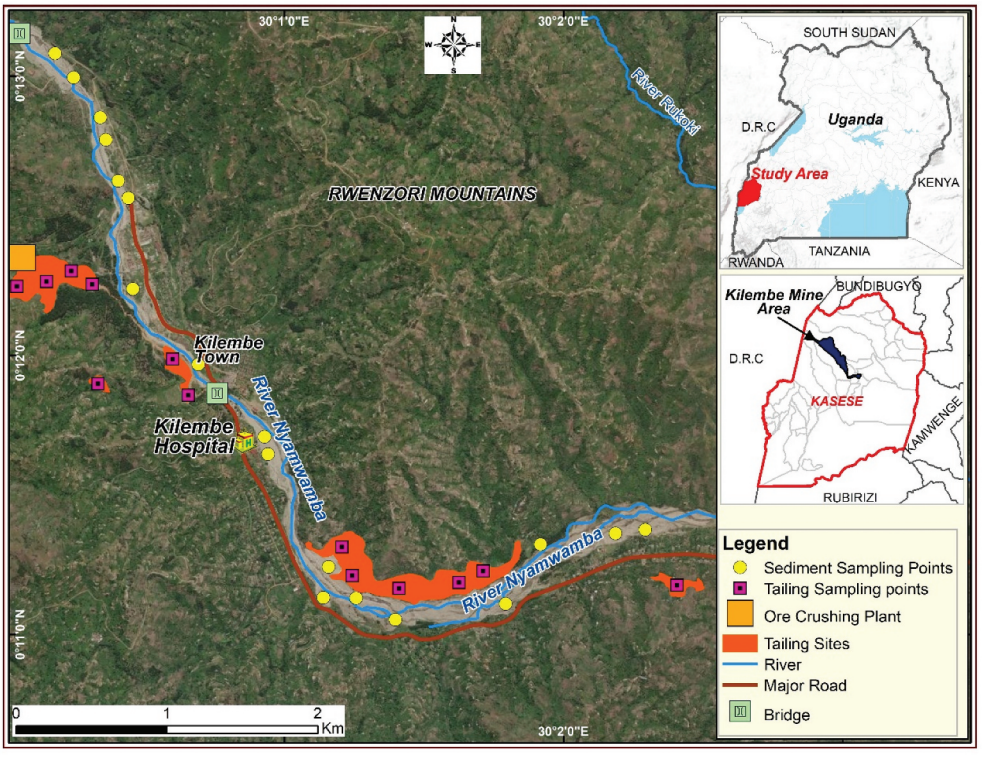

Figure 1. Kilembe mines, tailing sites, River Nyamwamba, and surrounding areas with locations of the sampling points, sediments (yellow dots), and tailings (purple squares).

covering more than 0.2 km^2, located on the bank of River Nyamwamba. The area's topology consists of mainly mountainous and hilly terrains and the river valley. The Kilembe mines area is densely populated, predominantly composed of the families of former mine workers, with the community largely dependent on subsistence farming for their livelihood. The most developed economic sector in the area is tourism.

Geologically, the Kilembe mines area is covered by a stratified sequence of metamorphic rocks known as the Kilembe series [18]. The rocks form part of the Kilembe schist belt within the Precambrian gneissic rocks and metamorphosed volcanic and sedimentary rocks south of the Rwenzori Mountain range. Kilembe mine rocks comprise major minerals such as pyrite, chalcopyrite, pyrrhotite, quartz and feldspar [19,20].

2.2. Sample collection and processing

In the present study, 31 samples, comprising 18 sediments and 13 tailings, were collected between October 2022 and March 2023 from Kilembe Valley along River Nyamwamba, as shown in Figure 1 with yellow dots (sediments) and purple squares (tailings). The sediment samples were collected using a hand coring tool down to 0–20 cm depth. The tailing samples were obtained from five mine tailing heaps along River Nyamwamba, with 4 to 5 cores randomly combined at each sampling point to create a composite sample of approximately 1.0 kg wet mass. This approach aimed to enhance sample representation and measurement reliability. Subsequently, the samples were sorted to remove foreign objects, placed in self-locking plastic bags, and coded for identification before transportation to the laboratory for processing and measurement. The samples were spread out on clean plastic sheets and sun-dried for 2–3 days in a low-background radiation area at the laboratory and then ground into fine powder using a stainless-steel electric grinder. The samples were then oven-dried at 105°C until there was no detectable change in weight. The samples were then sieved through a 2.0-millimetre mesh and homogenised to prevent low-energy self-absorption. The prepared samples were accurately weighed and packaged in 500 cm^3 Marinelli beakers, which were hermetically sealed using adhesive sellotape to prevent gas formic radon (^{222}Rn) escape. The beakers containing the samples were stored at room temperature for 30–35 days to allow radioactivity secular equilibrium between ^{226}Ra, ^{232}Th, and their daughter isotopes [21]. The samples were meticulously handled during sampling, processing and analysis to avoid cross-contamination.

2.3. Measurement of radionuclide concentrations

The ^{226}Ra, ^{232}Th, and ^{40}K radioactivity concentrations were analysed using a high-purity germanium (HPGe) detector (model GC-2018, Canberra), maintained at a liquid nitrogen temperature (77 K). A customised rectangular cage containing 5 cm thick lead blocks shielded the detector from background radiation interference. The cage has a 1.0 mm copper inner lining to attenuate the low-energy X-rays emitted by the lead blocks. The HPGe detector has a capacity of 104 cm^3, with a relative detection efficiency of 20% and a resolution of 1.8 keV (FWHM) for the 1.33 MeV gamma-ray emission line of ^{60}Co. Data acquisition and spectral peak fitting were executed using a computer-controlled multichannel analyser of the Canberra brand, coupled to the detector. The energy and detector

Table 1. Decay characteristics of the measured radionuclides.

Radionuclide of interest	Detectable radionuclide	Half-life (s)	γ-ray energy (keV)	Branching ratio (%)	Radionuclide source
^{226}Ra	^{214}Pb	1608	295.2	19.2	^{238}U(^{226}Ra) series
			351.9	37.2	
	^{214}Bi	1194	609.3	46.3	
^{232}Th	^{228}Ac	22140	1120.3	15.1	^{232}Th series
			1764.5	15.8	
			911.6	27.7	
			969.1	16.6	
^{40}K	^{212}Pb	38304	238.6	44.6	
	^{40}K	3.94×10^{16}	1460.8	10.7	Primordial

efficiency calibrations were performed using known standard point sources such as ^{60}Co and ^{137}Cs. The samples were counted for 6000 s, which was sufficient to obtain reasonable statistical uncertainties. The background radiation was measured using an empty sealed Marinelli beaker under identical experimental conditions as the samples. Subsequent spectral analyses and background radiation subtraction were performed using the Genie-2000 software package. The radioactivity concentrations of ^{226}Ra and ^{232}Th were determined by calculating the geometric mean of the activity concentrations of their daughter isotopes using the characteristic gamma lines listed in Table 1 [22]. The radioactivity concentration of ^{40}K was measured from its single gamma line at 1460.8 keV [14]. The activity concentration of the radionuclides in the analysed samples was determined utilising Equation (1) [14]:

$$A_i\left(\text{Bq kg}^{-1}\right) = \frac{N_i}{\eta(E) \times P_\gamma \times m \times t} \tag{1}$$

where $A_i(\text{Bq kg}^{-1})$ is the radionuclide activity concentration, N_i represents the net peak area (background corrected) of the respective full-energy peak, $\eta(E)$ represents detector efficiency relative to the photo peak energy, P_γ represents the absolute gamma emission transition probability, m represents the sample dry mass, and t is the measurement time (s). The minimum detectable activity was calculated from the peak areas of the background spectrum (B) at a 95% confidence level using Equation (2) [23,24]:

$$\text{MDA} = \frac{1.64 \times \sqrt{B}}{\eta(E) \times P_\gamma \times m \times t} \tag{2}$$

The minimum detectable activities for ^{226}Ra, ^{232}Th and ^{40}K in the samples were determined to be 1.8, 1.5 and 9.1 Bq kg^{-1}, respectively.

2.4. Radiological hazards and dose parameters

2.4.1. Radium equivalent activity

The uneven distribution of ^{226}Ra, ^{232}Th and ^{40}K in sediments and mine tailings significantly influences the radioactivity concentrations, much like in other environmental matrices. To evaluate the radiological risk to human health due to the different radionuclides in the samples, radium equivalent activity, Ra_{eq}, index is often used. This index provides a standardised measure by assuming that the specific activities of each of ^{226}Ra, ^{232}Th and ^{40}K produce an equal radiation dosage. The Ra_{eq} was evaluated using Equation (3), as

stated in [25]. For radiation exposure safety, the recommended upper limit of Ra_{eq} is 370 Bq kg^{-1}.

$$Ra_{eq} = A_{Ra} + 1.43A_{Th} + 0.077A_K \tag{3}$$

where A_{Ra}, A_{Th} and A_K are the mean radionuclide activity concentrations in Bq kg^{-1} of ^{226}Ra, ^{232}Th and ^{40}K, respectively.

2.4.2. Hazard indices

The external hazard index (H_{ex}) was calculated using Equation (4) [26] to assess the radiological hazard due to gamma radiation exposure from sediments and mine tailings.

$$H_{ex} = \frac{A_{Ra}}{370} + \frac{A_{Th}}{259} + \frac{A_K}{4810} \leq 1 \tag{4}$$

Similarly, the internal radiation exposure due to inhalation of airborne radioactive particles (mostly radon and its progenies) in the samples was assessed using the internal hazard index (H_{in}) according to Equation (5) [1,26]:

$$H_{in} = \frac{A_{Ra}}{185} + \frac{A_{Th}}{259} + \frac{A_K}{4810} \leq 1 \tag{5}$$

2.4.3. Gamma representative index

Considering the prevalent use of sediments and tailings as building materials in the Kilembe mines area, the gamma representative index, $\mathbf{I}_\gamma$, has been proposed as another parameter to assess the radiation hazard in these materials. This was calculated using Equation (6) [27]:

$$I_\gamma = \frac{A_{Ra}}{300} + \frac{A_{Th}}{200} + \frac{A_K}{3000} \leq 1 \tag{6}$$

2.4.4. Absorbed dose rates

The outdoor absorbed radiation dosage $D_{out}\left(nGyh^{-1}\right)$ received by human beings in air at a height of 1 metre above the ground level was estimated using Equation (7), as reported in [23]:

$$D_{out}\left(nGyh^{-1}\right) = 0.427A_{Ra} + 0.662A_{Th} + 0.0432A_K \tag{7}$$

The indoor absorbed dosage $D_{in}\left(nGyh^{-1}\right)$ was evaluated according to Equation (8) [28]:

$$D_{in}\left(nGyh^{-1}\right) = 0.92A_{Ra} + 1.1A_{Th} + 0.08A_K \tag{8}$$

2.4.5. Annual effective dose

The annual effective dose from gamma radiation outdoor (E_{out}) and indoor (E_{in}) exposures were determined based on the absorbed radiation dose rates. Typically, residents spend 20% of their time outdoors and the remaining 80% indoors. Accordingly, the occupancy factors were set at 0.2 and 0.8 for external and indoor radiation exposures, respectively.

Equations (9) and (10)were used to calculate E_{out} and E_{in}, with 0.7 Sv Gy^{-1} as a conversion factor [27,28]:

$$E_{out}\left(mSvy^{-1}\right) = D_{out}\left(nGyh^{-1}\right) \times 0.7\left(Sv\ Gy^{-1}\right) \times 0.2 \times 8760\left(hy^{-1}\right) \times 10^{-6} \quad (9)$$

$$E_{in}\left(mSvy^{-1}\right) = D_{in}\left(nGyh^{-1}\right) \times 0.7\left(Sv\ Gy^{-1}\right) \times 0.8 \times 8760\left(hy^{-1}\right) \times 10^{-6} \quad (10)$$

2.4.6. Excess lifetime cancer risk

To evaluate the probability that an individual continuously exposed to a specified radiation level would develop cancer, a parameter known as excess lifetime cancer risk (ELCR) is often used. Outdoor and indoor ELCR associated with the gamma radiation from sediments and mine tailings were evaluated using Equations (11) and (12) [29]:

$$ELCR_{out} = E_{out} \times R_f \times A_{lt} \times 10^{-3} \quad (11)$$

$$ELCR_{in} = E_{in} \times R_f \times A_{lt} \times 10^{-3} \quad (12)$$

where R_f is the stochastic cancer risk factor, set at 0.05 Sv^{-1} for the general public, and A_{lt} is the average lifespan expectancy, taken as 70 years in this study. [1]

2.5. Statistical analysis

Data processing and statistical analysis were performed using Origin (version 2018). Pearson's correlation coefficient and hierarchical cluster analysis were used to exhibit and identify patterns in the relationship between the measured radioactivity concentrations and the estimated radiological hazards.

3. Results and discussion

3.1. Radionuclide activity concentrations

The statistical summary (mean ± SD, minimum and maximum) of ^{226}Ra, ^{232}Th, and ^{40}K activity concentrations in sediments and tailing samples is presented in Table 2 (full details are provided in Tables S1 and S2, Supplementary Information). The mean activity concentrations of ^{226}Ra, ^{232}Th and ^{40}K in sediments were 38.6, 37.4, and 708.0 Bq kg^{-1}, respectively. In the case of tailings, the mean activity concentrations were 171.3, 34.8, and

Table 2. Radioactivity concentrations in sediments and mine tailings.

			Radioactivity concentration (Bq kg^{-1})		
Sample	No.		^{226}Ra	^{232}Th	^{40}K
Sediments	18	Min	28.4	21.1	455.3
		Max	56.9	48.9	1040.0
		Mean ± SD	38.6 ± 8.9	37.4 ± 7.8	708.0 ± 147.3
Tailings	13	Min	102.7	16.1	436.2
		Max	212.4	63.6	1176.4
		Mean ± SD	171.3 ± 31.7	34.8 ± 14.9	792.4 ± 208.2

SD: standard deviation.

792.4 Bq kg^{-1} for ^{226}Ra, ^{232}Th and ^{40}K, respectively. The mean activity concentrations of ^{226}Ra and ^{40}K in tailings were higher than those in sediments. The mean radionuclide activity concentrations in both sediments and tailing samples followed the order ^{232}Th < ^{226}Ra < ^{40}K. The high specific activity of ^{40}K compared to ^{226}Ra and ^{232}Th signifies the relative natural abundance of potassium in igneous and metamorphic rocks, which are commonly associated with copper deposits [30]. Moreover, minerals such as quartz and feldspar that accumulate ^{40}K over time have been documented in the Kilembe mines area, as reported in the relevant literature [19,20]. According to UNSEAR, the global average activity concentrations of radionuclides ^{226}Ra, ^{232}Th, and ^{40}K are 35, 30, and 400 Bq kg^{-1}, respectively [1]. It was observed that the mean activity concentrations of ^{226}Ra and ^{232}Th in sediments were slightly higher than the world average values whereas that of ^{40}K was significantly higher than the UNSEAR value. In tailing samples, the mean activity concentration of ^{226}Ra and ^{40}K were significantly higher than the global average values whereas that of ^{232}Th was close to the UNSEAR value. The high activity concentration of ^{226}Ra observed in the tailing samples is likely attributed to the presence of uranium-rich minerals such as uraninite and monazite commonly found in copper ores [31]. Given that ^{226}Ra is a decay product of ^{238}U, its abundance in the copper mine tailings would be expected due to the mineral composition of the ore. Nevertheless, the high radionuclide activity concentrations in both sediments and tailing samples can generally be attributed to several factors including erosion, weathering of rocks, clay minerals, and mining by-products at specific places in the study area. Furthermore, higher concentrations of heavy metals like cobalt, copper, nickel and lead were reported in soil and mine tailings within the study area [17,32]. Heavy metals can contribute to increased radionuclide mobility, potentially influencing their concentrations [33].

As can be observed in Figure 2, there was heterogeneity in the concentration of radionuclides in both the sediments and tailing samples, which could be due to the geological and geochemical mineralisation disparities in the Kilembe copper mines area [17,20].

The radionuclide activity concentrations in our samples were compared with those reported in other countries, as presented in Table 3. The mean activity concentration of ^{226}Ra in sediments was lower than those reported in other countries, except Iraq,

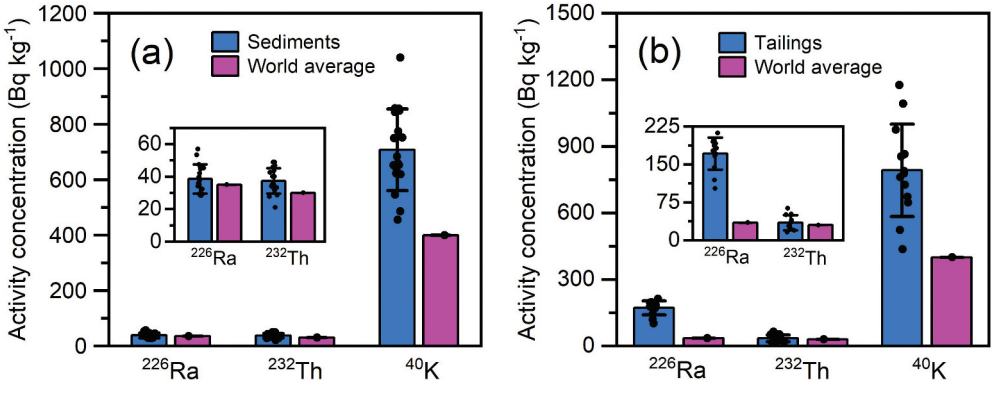

Figure 2. Radioactivity concentrations of ^{226}Ra, ^{232}Th and ^{40}K in (a) sediments and (b) tailings. Insets show zoomed ^{226}Ra and ^{232}Th activity concentrations. Dots represent individual data sampling points (18 sediments and 13 tailings), and bars represent mean ± SD.

Table 3. Average radioactivity concentrations in sediment and tailing samples from different countries.

Country	Sample	Detector	Radioactivity concentration (Bq kg^{-1})			Reference
			^{226}Ra	^{232}Th	^{40}K	
India	Sediments	NaI(Tl)	40.8	51.8	838.1	[34]
Vietnam	Sediments	HPGe	59.4	83.4	681.0	[13]
Iraq	Sediments	NaI(Tl)	9.9	23.1	232.9	[35]
Italy	Sediments	HPGe	20.8	36.4	907.1	[12]
Greece	Sediments	HPGe	42.0	28.0	480.0	[11]
Namibia	Sediments	HPGe	175.5	40.1	349.6	[36]
Bangladesh	Sediments	HPGe	23.7	37.2	445.1	[37]
Uganda	Sediments	HPGe	38.6	37.4	708.0	This study
South Africa	Tailings	BEGe	485.3	43.9	427.0	[14]
Nigeria	Tailings	ICPMS	86.3	64.5	1133.0	[38]
Peru	Tailings	NaI(Tl)	11.5	8.8	497.1	[16]
Portugal	Tailings	BEGe	158.0	32.2	917.0	[39]
Kenya	Tailings	NaI(Tl)	84.0	123.0	263.0	[10]
Uganda	Tailings	HPGe	171.3	34.8	792.4	This study

HPGe: high purity germanium detector, NaI(Tl): thallium activated sodium iodide detector, ICPMS: inductively coupled plasma mass spectrometer, and BEGe: broad energy germanium detector.

Bangladesh and Italy. For ^{232}Th, the mean value was higher or comparable with those in Iraq, Greece, Bangladesh and Italy but lower than the values reported in other countries (Table 3). The mean activity concentration of ^{40}K was higher than those reported in the listed countries, except India and Italy. In tailings, the mean activity concentration of ^{226}Ra was higher than the values reported in other countries except South Africa (Table 3). The mean activity concentration of ^{232}Th was lower than the values documented in most countries except Peru and Portugal. For ^{40}K, the mean activity concentration was higher than the ones reported in previous studies in Kenya, South Africa and Peru but lower than those from Nigeria and Portugal. The observed discrepancies in the radionuclide activity concentrations reported in different countries can be attributed to the differences in the geological formations and mineral compositions. In addition, mining techniques, ore raw materials and extraction processes vary from country to country, which may influence the distribution and concentration of radionuclides.

3.2. Radiological hazard parameters

The associated radiological hazard parameters were calculated to estimate the dose impact of radionuclides in sediments and tailings on human health. The statistical summary of the radiological hazard parameters is presented in Table 4 (full details are provided in Tables S3 and S4, Supplementary Information). The average radium equivalent activity (Ra_{eq}) in sediments was 146.5 Bq kg^{-1}. Meanwhile, in tailings, the mean Ra_{eq} value was 282.1 Bq kg^{-1}. These values closely align with those reported previously, such as a study in river sediments from India, where the mean Ra_{eq} value was 179.6 Bq kg^{-1} [34], and a gold mine tailings study from Nigeria, where the average Ra_{eq} value was 238.5 Bq kg^{-1} [38]. More importantly, the mean Ra_{eq} values in the present study's sediments and tailing samples were below the internationally recommended upper limit of 370 Bq kg^{-1} (Figure 3(a); Table 4).

Table 4. Calculated radiological hazard parameters associated with the measured radioactivity concentrations in sediments and tailing samples. SD is the standard deviation, and PL is the permissible limit.

				Hazard indices			D (nGy h^{-1})		E (mSv y^{-1})			ELCR $\times 10^{-3}$		
Sample type	No.		Ra_{eq}	H_{ex}	H_{in}	I_γ	D_{out}	D_{in}	E_{out}	E_{in}	E_T	$ELCR_{out}$	$ELCR_{in}$	$ELCR_t$
Sediments	18	Min	104.5	0.28	0.37	0.4	51.3	96.6	0.06	0.47	0.54	0.22	1.66	1.88
		Max	192.8	0.52	0.67	0.72	93.7	174.6	0.11	0.86	0.97	0.4	3	3.4
		Mean ± SD	146.5 ± 26.1	0.4 ± 0.07	0.5 ± 0.09	0.55 ± 0.10	71.8 ± 12.7	133.2 ± 28.3	0.09 ± 0.02	0.65 ± 0.12	0.74 ± 0.12	0.31 ± 0.05	2.29 ± 0.41	2.6 ± 0.41
Tailings	13	Min	229.9	0.62	0.92	0.84	108.1	211.2	0.13	1.04	1.17	0.46	3.63	4.09
		Max	345	0.93	1.46	1.25	162.1	317.2	0.2	1.56	1.76	0.7	5.45	6.14
		Mean ± SD	282.1 ± 39.7	0.76 ± 0.11	1.23 ± 0.17	1.01 ± 0.14	130.4 ± 18.4	259.3 ± 35.4	0.16 ± 0.02	1.27 ± 0.17	1.43 ± 0.17	0.56 ± 0.08	4.45 ±0.61	5.01 ± 0.61
		P.L	370	≤1	≤1	≤1	59	84	0.07	0.41	0.48	0.29	1.16	1.45

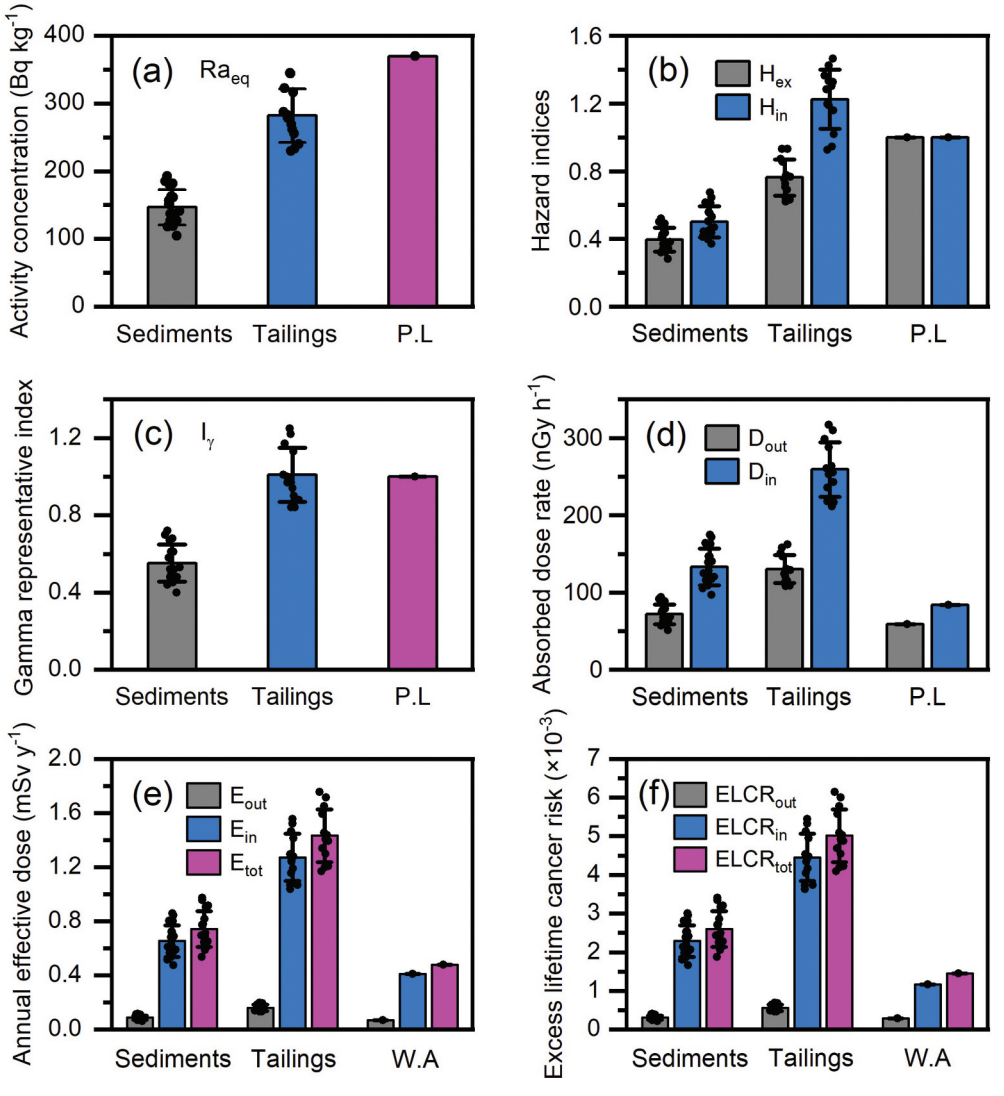

Figure 3. Calculated radiological hazard parameters due to radionuclides in sediments and tailing samples. (a) Radium equivalent activity, (b) hazard indices, (c) gamma representative index, (d) radiation absorbed dose rates, (e) annual effective dose rates and (f) excess lifetime cancer risk. Dots: individual data sampling points (18 sediment and 13 tailing samples), bars: mean ± SD, PL: permissible limit and WA: world average.

The mean values of external (H_{ex}) and internal (H_{in}) hazard indices in sediments were 0.40 and 0.50, respectively. These values were below the global averages, suggesting that sediments pose minimal hazardous effects. Conversely, the mean H_{ex} and H_{in} values were 0.76 and 1.23 for tailings, respectively. While the mean H_{ex} was below the permissible limit for public exposure, H_{in} was greater than the internationally recommended unity value (Figure 3(b); Table 4). Consequently, the potential health hazards due to internal radiation

exposure through ^{222}Rn gas and its progenies cannot be overlooked, making the tailings unsuitable for use as building materials.

The calculated mean value of the gamma representative index, I_γ, in sediments was 0.55. While in tailings, the mean I_γ value was 1.01, slightly exceeding the global average permissible limit (Figure 3(c); Table 4). Additionally, 38% of the sampled tailings showed I_γ values greater than unity.

The calculated average outdoor radiation dose rate (D_{out}) for sediments was 71.8 nGy h^{-1}, while the indoor dose rate (D_{in}) was 133.2 nGy h^{-1} (Figure 3(d); Table 4). It is worth pointing out that 83% of the sampled sediments had D_{out} values higher than the global average of 59 nGy h^{-1}, recommended by UNSCEAR [1]. Additionally, in all the sediment samples, the D_{in} values exceeded the recommended limit of 84 nGy h^{-1} [1]. The average D_{out} value in tailings was 130.4 nGy h^{-1}, while the D_{in} value was 259.3 nGy h^{-1}. These values were higher than the recommended permissible limits of 59 and 84 nGy h^{-1} for D_{out} and D_{in} by 2.2 and 3.1 times, respectively. These elevated dose rates are indicators of the unsuitability of the sampled tailings as construction materials.

The average annual effective dose (E_{out}) from outdoor gamma radiation, calculated for sediments, was 0.09 mSv y^{-1}, and the indoor dose (E_{in}) was 0.65 mSv y^{-1} (Figure 3(e); Table 4). Most of the sampled sediments exhibited E_{out} and E_{in} values greater than the global average limits of 0.07 and 0.41 mSv y^{-1}, respectively. This demonstrates that prolonged exposure to gamma radiation from these sediments could pose health risks. However, the total effective dose in individual samples was less than the safety limit of 1 mSv y^{-1} [40]. Therefore, these sediments could still be used in construction materials under regulated conditions. The average E_{out} resulting from gamma radiation in tailing samples was 0.16 mSv y^{-1}, while the mean E_{in} value was 1.27 mSv y^{-1} (Figure 3(e); Table 4). The mean E_{out} and E_{in} values were 2.3 and 3.1 greater than the global average limits of 0.07 and 0.41 mSv y^{-1}, respectively. Moreover, for all the individual tailing samples, the sum of E_{out} and E_{in} exceeded the safe dose criterion of 1 mSv y^{-1} [40]. This further indicates that the sampled mine tailings are unsafe for construction materials.

The average outdoor excess lifetime cancer risk ($ELCR_{out}$) in sediments was 0.31×10^{-3}, while the indoor ($ELCR_{in}$) was 2.29×10^{-3} (Figure 3(f); Table 4). The total excess lifetime cancer risk ($ELCR_t$) was 2.60×10^{-3}. These mean $ELCR_{out}$, $ELCR_{in}$ and $ELCR_t$ values exceeded the recommended values of 0.29×10^{-3}, 1.16×10^{-3} and 1.45×10^{-3} by 1.1, 2.0 and 1.8 times, respectively [41]. On the other hand, the $ELCR_{out}$ average value in tailings was 0.56×10^{-3}. The mean $ELCR_{in}$ value was 4.45×10^{-3}, while the mean $ELCR_t$ value was 5.01×10^{-3}. The mean $ELCR_{out}$, $ELCR_{in}$ and $ELCR_t$ values in tailing samples were higher than the recommended values of 0.29×10^{-3}, 1.16×10^{-3} and 1.45×10^{-3} by 1.9, 3.8 and 3.5 times, respectively [41]. The elevated mean $ELCR_t$ values observed in both sediments and tailings indicate an increase in the likelihood of developing cancer for individuals residing in buildings constructed using these materials, depending on the exposure time.

3.3. Statistical analysis

We performed a Pearson correlation analysis to understand the relationship between the measured radioactivity concentrations and the estimated radiological hazard parameters. The Pearson correlation coefficients were categorised into weak (0.00–0.39), moderate (0.40–0.59), strong (0.60–0.79), and very strong (0.80–1.00) correlations [42]. A significance level of 0.01 was applied for this analysis. As manifested in Figure 4(a), all the variables in the analysed sediment samples originate from similar natural sources. However, a moderate correlation between ^{40}K and ^{232}Th indicates that these radionuclides may be influenced by slightly different natural processes [43]. In addition, very strong correlations exist between the radioactivity of ^{226}Ra, ^{232}Th, and ^{40}K with the computed radiological hazard parameters, along with very strong correlations among the radiological hazard parameters themselves. This indicates that ^{226}Ra, ^{232}Th, and ^{40}K are pivotal in the radiological hazards and subsequent risks to human health, mainly from the gamma radiation emitted by natural radionuclides in the analysed samples.

Figure 4(b) displays the Pearson correlation between the radionuclides measured in tailings and concomitant radiological hazard parameters. Notably, distinct associations among the radionuclides were observed in the tailings. Specifically, ^{232}Th and ^{40}K showed a weak negative correlation with ^{226}Ra. The negative correlation between ^{40}K and ^{226}Ra is explained by the fact that ^{40}K does not originate from the decay chains of ^{238}U and ^{232}Th [22,44]. Rather, as a naturally occurring radioactive isotope, ^{40}K undergoes independent decay, resulting in a weak correlation with other radionuclides in the samples.

Similarly, ^{226}Ra and ^{232}Th exhibited a weak negative correlation. This observation can be attributed to geochemical heterogeneity and differential mobility patterns of ^{226}Ra and ^{232}Th in the tailing's complex matrix. Moreover, these two radionuclides belong to different decay chains. The calculated radiological hazard parameters in

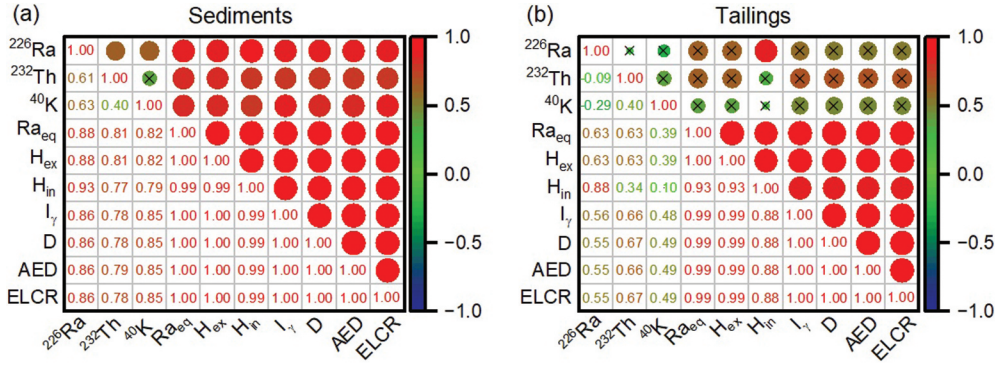

Figure 4. The heatmap visualisation of Pearson correlation analysis between radioactivity concentrations and the concomitant radiological hazard parameters in (a) sediment and (b) tailing samples. Positive correlations are indicated in red, while negative correlations are in blue. The colour's intensity reflects the correlation's strength, with darker colours indicating stronger associations. Circle size corresponds to correlation strengths, with smaller circles indicating weaker correlations. The Pearson correlation coefficients are indicated in the lower triangular part.

tailings generally showed a moderate to strong correlation with ^{226}Ra and ^{232}Th. An exception was H_{in}, which manifested a stronger correlation with ^{226}Ra and a weaker correlation with ^{232}Th. Meanwhile, a moderate to weak association with radiological parameters was observed for ^{40}K, which suggests that this particular radionuclide has negligible influence on the radiological risks due to gamma radiation exposure from tailings.

Hierarchical cluster analysis (HCA) effectively identifies patterns and connections between the radioactivity in the analysed samples and the radiological hazard parameters. HCA consists of a set of multivariate algorithms that recursively group similar variables in the same cluster. The most similar variables are grouped first, and the process continues until all the data is organised into clusters based on their similarity. A dendrogram is constructed based on the degree of similarity, where 100% indicates zero linkage distance between the respective variables, and 0% denotes the maximal linkage distance (dissimilar variables). Figure 5 illustrates dendrograms for the analysed samples. Within both sediments and tailings, three distinct clusters were identified. In Figure 5(a), cluster I comprise ^{226}Ra and the radiological hazard parameters. Cluster II, linked to cluster I, consists of ^{40}K, while cluster III contains ^{232}Th.

Similarly, in tailings, cluster I comprises ^{226}Ra and the radiological hazard parameters (Figure 5(b)). Cluster II consists of ^{232}Th, while ^{40}K is in Cluster III at a significantly longer linkage distance. This observation implies that ^{40}K has minimal contribution to the radiological hazards in the tailing samples. Importantly, the HCA results are qualitatively in agreement with the Pearson correlation analysis.

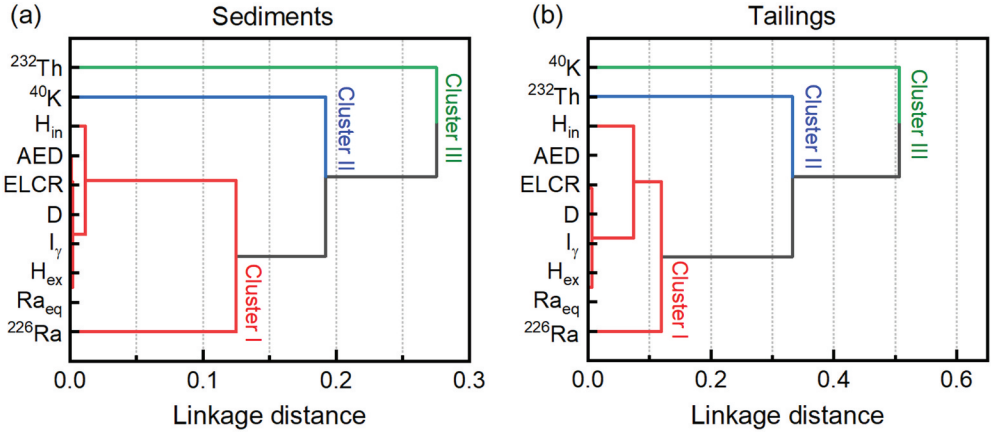

Figure 5. Dendrograms for the hierarchical cluster analysis exhibiting the patterns in the correlation between the measured radionuclides and the radiological hazard parameters in (a) sediment and (b) tailing samples.

4. Conclusion

This study assessed the activity concentrations of ^{226}Ra, ^{232}Th and ^{40}K and associated radiological hazards such as Ra_{eq}, H_{ex}, H_{in}, I_{γ}, D_{out}, D_{in}, E_{out} E_{in}, $ELCR_{out}$ and $ELCR_{in}$ in sediments and tailings from the Kilembe copper mines area using an HPGe gamma-ray spectrometer. The results were compared with the global average values according to UNSCEAR 2000. In sediments, the mean activity concentrations of ^{226}Ra and ^{232}Th were close to the global average values whereas that of ^{40}K was higher than the global average value. The mean activity concentrations of ^{226}Ra and ^{40}K in tailings were significantly higher than the global average values whereas that of ^{232}Th was similar to the global average value. The majority of the calculated radiological hazard parameters in sediments were above the world's average values, except Ra_{eq}, I_{γ}, H_{ex} and H_{in}. While in tailings, all the hazard parameters surpassed the global average values except Ra_{eq} and H_{ex}. Consequently, using these sediments and tailings for construction or domestic utensil cleaning by the local community in the Kilembe copper mines is unsafe. Statistical analysis suggested that ^{226}Ra is the main contributor to the assessed radiological hazards in the analysed samples.

4.1. Recommendations

The study findings suggest that there is a need for:

- Assessing the actual risks to human health due to natural radionuclides and possible remediations for safely using sediments and tailings as building materials.
- Assessing the radionuclide concentrations in water, soil, and plants around the Kilembe copper mines area.
- Evaluating the concentration of radon in the construction materials, such as bricks and blocks used in the Kilembe area. This evaluation will contribute to understanding the potential radiation exposure pathways in the study area.
- Establishment of appropriate action measures for the effective management and utilisation of sediments and tailings in the area. These measures are important for ensuring the safety and well-being of the local population and the environment.

Acknowledgments

We acknowledge UISTF for the scholarship and Kyambogo University for providing equipment, support, and space to conduct the experiments at the Radiation Laboratory in the Department of Physics. The authors also wish to appreciate the Uganda Atomic Energy Council for providing the research clearance certificate that ethically and legally made it possible to conduct the study.

Disclosure statement

No potential conflict of interest was reported by the author(s).

ORCID

Evarist R. S. Turyahabwa http://orcid.org/0009-0001-8778-093X
Farooq Kyeyune http://orcid.org/0000-0002-9033-9854
Manny Mathuthu http://orcid.org/0000-0001-7608-2610

Author contributions

ERST: Conceptualisation, data curation, methodology, data analysis, software and original manuscript writing. FK: Data visualisation, interpretation, manuscript writing, and editing. E. M: Conceptualisation and supervision. A.K: Conceptualisation and supervision. MM: advised on formal data analysis. All authors have reviewed the manuscript and consented to its publication.

References

[1] United Nations Scientific Committee on the Effects of Atomic Radiation, Report No. 9210582489, 2000.
[2] A. Del Carmen Arriola-Velásquez, A. Tejera, H. Alonso, N. Miquel-Armengol, J.G. Rubiano, P. Martel, Environ. Pollut. **340**, 122809 (2024). doi:10.1016/j.envpol.2023.122809.
[3] R. Sabeeh Ahmed, J. Radiat. Res. Appl. Sci. **15**, 245 (2022). doi:10.1016/j.jrras.2022.03.012.
[4] A. Ahmed Qureshi, S. Tariq, K. Ud Din, S. Manzoor, C. Calligaris and A. Waheed, J. Radiat. Res. Appl. Sci. **7** (4), 438 (2014). doi:10.1016/j.jrras.2014.07.008; A.E. Abdel Gawad, H. Eliwa, M.S. Masoud, M.U. Khandaker, M.Y. Hanfi, Sci. Rep. **13**, 21202 (2023).
[5] A. Faanu, O.K. Adukpo, L. Tettey-Larbi, H. Lawluvi, D.O. Kpeglo, E.O. Darko, G. Emi-Reynolds, R. A. Awudu, C. Kansaana, P.A. Amoah, A.O. Efa, A.D. Ibrahim, B. Agyeman, R. Kpodzro and L. Agyeman, Springerplus **5**, 1 (2016). doi:10.1186/s40064-016-1716-5.
[6] A. Nikvar-Hassani, H. Vashaghian, R. Hodges and L. Zhang, Constr. Build. Mater. **324**, 126695 (2022). doi:10.1016/j.conbuildmat.2022.126695.
[7] N. Zhang, B. Tang and X. Liu, Constr. Build. Mater. **288**, 123022 (2021). doi: 10.1016/j.conbuildmat.2021.123022.
[8] Z. Wei, J. Zhao, W. Wang, Y. Yang, S. Zhuang, T. Lu and Z. Hou, Constr. Build. Mater. **282**, 122655 (2021). doi:10.1016/j.conbuildmat.2021.122655.
[9] E. Klubi, J.M. Abril, J. Mantero, R. García-Tenorio and E. Nyarko, J. Environ. Radioact. **218**, 106260 (2020). doi:10.1016/j.jenvrad.2020.106260.
[10] C.K. Wanyama, F.W. Masinde, J.W. Makokha and S.M. Matsitsi, Radiat. Prot. Dosimetry. **190** (3), 324 (2020). doi:10.1093/rpd/ncaa113.
[11] F.K. Pappa, C. Tsabaris, A. Ioannidou, D.L. Patiris, H. Kaberi, I. Pashalidis, G. Eleftheriou, E.G. Androulakaki and R. Vlastou, Appl. Radiat. Isot. **116**, 22 (2016). doi:10.1016/j.apradiso.2016.07.006.
[12] F. Caridi, S. Marguccio, M. D'Agostino, A. Belvedere and G. Belmusto, Eur. Phys. J. Plus **131** (5) (2016). doi:10.1140/epjp/i2016-16155-x.
[13] V.-H. Duong, D.-T. Duong L. Van Bui, Tran TD, Phan TT, Nguyen TD, Arch. Environ. Contam. Toxicol. **85** (3), 302 (2023). doi:10.1007/s00244-023-01003-3
[14] C. Kamunda, M. Mathuthu and M. Madhuku, Int. J. Environ. Res. Public Health **13**, 138 (2016). doi:10.3390/ijerph13010138.
[15] A.T. William Rabuku and A.Q. Malik, Renew. Energy Environ. Sustain. **5**, 10 (2020). doi:10.1051/rees/2020005.
[16] R. Liza, P. Pereyra, J. Rau, M. Guzman, L. Sajo-Bohus and D. Palacios, Atmosphere **14**, 588 (2023). doi:10.3390/atmos14030588.
[17] A.R. Mwesigye, S.D. Young, E.H. Bailey and S.B. Tumwebaze, Sci. Total Environ. **573**, 366 (2016). doi:10.1016/j.scitotenv.2016.08.125.

[18] F.U. Bauer, M. Karl, U.A. Glasmacher, B. Nagudi, A. Schumann and L. Mroszewski, JAfES **73**, 44 (2012). doi:10.1016/j.jafrearsci.2012.07.001.
[19] M.R. Abraham and T.B. Susan, Chemosphere **169**, 281 (2017). doi:10.1016/j.chemosphere.2016.11.077.
[20] T. Hartwig, M. Owor, A. Muwanga, D. Zachmann and W. Pohl, Mine Water Environ. **24**, 114 (2005). doi:10.1007/s10230-005-0082-2.
[21] M. Zivuku, N. Anna Kgabi and V. Makondelele Tshivhase, Sci. Afr. **20**, e01722 (2023). doi:10.1016/j.sciaf.2023.e01722; F. Lolilaand M.S. Mazunga, J. Radiat. Res. Appl. Sci. **16**, 100524 (2023).
[22] M.M. Mahfuz Siraz M.A. Jubair Al Mahmud Alam MS, Das SC, Bradley DA, Khandaker MU, Tokonami S, Shelley A, Yeasmin S., Int. J. Environ. Anal. Chem. **1**, 13(2023).
[23] M.M. Mahfuz Siraz, M.J. Dewan, M.I.A. Chowdhury, J. Al Mahmud, M.S. Alam, M.B. Rashid, N. Sultana, M.F. Kabir, M.U. Khandaker and S. Yeasmin, Int. J. Environ. Anal. Chem. **1** (2023). doi:10.1080/03067319.2023.2196021.
[24] S. Biira, P. Ochom and B. Oryema, J. Environ. Radioact. **227**, 106460 (2021). doi:10.1016/j.jenvrad.2020.106460.
[25] S. Yeasmin, S. K. Das, M. M. Siraz and M. S. Rahman, Int. J. Environ. Anal. Chem. 1–18. (2023). doi:10.1080/03067319.2023.2267995.
[26] S. Penabei, D. Bongue, H. Eyakifama, A. Ngwa Ebongue, A. Mistura Bolaji, M. Peane, C. J. Guembou Shouop, J.C. Brigui Olkalé, H. Yacoub Idriss and M.G. Kwato Njock, Int. J. Environ. Anal. Chem. **1** (2023). doi:10.1080/03067319.2022.2152687.
[27] S. Amatullah, R. Rahman, J. Ferdous, M.M.M. Siraz, M.U. Khandaker and S.F. Mahal, Int. J. Environ. Anal. Chem. **103**, 3376 (2023). doi:10.1080/03067319.2021.1907361.
[28] M.M. Abd Elkader, T. Shinonaga and M.M. Sherif, Sci. Rep. **11**, 23251 (2021). doi:10.1038/s41598-021-02559-7.
[29] E.H. Abdelfadeel, E.S. Abd El-Halim, T.M. Hegazy and H.A.A. Ghany, Sci. Rep. **13** (1), 10952 (2023). doi:10.1038/s41598-023-37403-7 ;International Commission on Radiological Protection, Report No. 0080215114, 1990.
[30] H. El-Gamal, A. Sefelnasr and G. Salaheldin, Water **11**, 311 (2019). doi:10.3390/w11020311.
[31] M. Rollog, N.J. Cook, P. Guagliardo, K.J. Ehrig and M. Kilburn, Hydrometallurgy **190**, 105153 (2019). doi:10.1016/j.hydromet.2019.105153
[32] A.R. Mwesigye and O.B. Lawrence, Soil. Sediment. Contam. **1**, (2023). doi:10.1080/15320383.2023.2195512.
[33] N. Tamannaya Dina, S. Chandra Das, M. Zafrul Kabir, M.G. Rasul, F. Deeba, M. Rajib, M.S. Islam, M.A. Hayder and M.I. Ali, J. Radioanal. Nucl. Chem. **331**, 4457 (2022). doi:10.1007/s10967-022-08562-0.
[34] V. Thangam, A. Rajalakshmi, A. Chandrasekaran and B. Jananee, Int. J. Environ. Anal. Chem. **102**, 422 (2022). doi:10.1080/03067319.2020.1722815.
[35] T. Yaseen Wais and L.A. Najam, J. Phys. Conf. Ser. **1999**, 012064 (2021). doi:10.1088/1742-6596/1999/1/012064.
[36] S.A. Onjefu, S.H. Taole, N.A. Kgabi, C. Grant and J. Antoine, J. Radiat. Res. App. Sci. **10**, 301 (2017). doi:10.1016/j.jrras.2017.07.003.
[37] A.A.M. Sirajul Islam, M.M.H. Miah, M. Ahmed, S. Hossain and M.U. Khandaker, Int. J. Environ. Anal. Chem. **103**, 3779 (2023). doi:10.1080/03067319.2021.1912339.
[38] T.A. Laniyan and A.J. Adewumi, Environ. Earth Sci. **80**, 375 (2021). doi:10.1007/s12665-021-09674-8.
[39] I. Paiva, R. Marques, M. Santos, M. Reis, M.I. Prudêncio, J.C. Waerenborgh, M.I. Dias, D. Russo, G. Cardoso, B.J.C. Vieira, E. Carvalho, C. Rosa, D. Lobarinhas, C. Diamantino and R. Pinto, Chemosphere **223**, 171 (2019). doi:10.1016/j.chemosphere.2019.02.057.
[40] European Commission, *Radiological Protection Principles Concerning the Natural Radioactivity of Building Materials* (European Commission, Brussels, 1999).
[41] S. Abdullahi, A. Fazli Ismail and S. Samat, Nucl. Eng. Technol. **51**, 325 (2019). doi:10.1016/j.net.2018.09.017.

[42] M.J. Abedin, M.R. Karim, M. Uddin Khandaker, M. Kamal, S. Hossain, M.H.A. Miah, D.A. Bradley, M.R.I. Faruque and M.I. Sayyed, Radiat. Phys. Chem. **177**, 109165 (2020). doi:10.1016/j.radphyschem.2020.109165.

[43] A.E. Abdel Gawad, K. Ali, H. Eliwa, M.I. Sayyed, M.U. Khandaker, D.A. Bradley, H. Osman, B. H. Elesawy and M.Y. Hanfi, Appl. Sci. **11**, 11884 (2021). doi:10.3390/app112411884.

[44] U. Azeem, H. Younis, K. Mehboob, M. Ajaz, M. Ali, A. Hidayat, W. Muhammad, Nucl. Eng. Technol. 56, 207 (2023).